Frequency downshift in rapidly ionizing media

S. P. Kuo and A. Ren
Weber Research Institute and Department of Electrical Engineering, Polytechnic University, Route 110, Farmingdale, New York 11735

G. Schmidt
Department of Physics and Engineering Physics, Stevens Institute of Technology, Hoboken, New Jersey 07030
(Received 16 July 1993)

It is known that an electromagnetic wave propagating in a rapidly ionizing medium undergoes a frequency upshift. Here experimental evidence and theory are presented for the simultaneous creation of a downshifted wave. There is excellent agreement between experimental results and computer simulation based on a simple theory.

PACS number(s): 52.40.Db, 52.70.Gw, 84.40.Cb

Recently, theory and computer simulation [1–6] and experiments [7–14] have demonstrated that the frequency of an electromagnetic (EM) wave interacting with a rapidly created plasma is upshifted. The underlying physics can be realized by the fact that after the sudden increase of the plasma density, the wave experiences only a temporal variation of the plasma, and the wavelength $\lambda_0=2\pi/k_0$ of the wave does not change. However, the rapidly created plasma causes a sudden reduction on the index of refraction $\sqrt{\varepsilon_r}$ of the background medium and forces the wave to propagate with a larger phase velocity. Hence, the new wave has to oscillate with higher angular frequency $\omega=(\omega_0^2+\omega_{pe}^2)^{1/2}$ at the subsequent time in order to satisfy the dispersion relation $\varepsilon_r=k_0^2c^2/\omega^2$, where ω_0 and ω_p are the initial frequency of the wave and the plasma frequency, respectively.

The interest in the frequency upshifting phenomenon can be attributed to its many potential applications, including the enhancement of the frequency tuning capability of existing sources of EM waves [9] and improvement of the performance of high-power radar and direct energy systems by enabling reflectionless propagation of very powerful microwave pulses through the air [15,16], etc. Moreover, there are no technical difficulties in producing dense plasma rapidly.

It was observed that in some experiments [7,12] a frequency downshift also exists. Since the created plasma decayed much more slowly than it grew and since the frequency downshift lines did not appear in the results of computer simulations using a lossless unmagnetized plasma model [1], the frequency downshift phenomenon has not been discussed. On the other hand, when a magnetized plasma is considered, a new branch of EM mode in the low frequency regime emerges and it has been shown that part of the wave energy is converted into that of this low frequency mode after a sudden increase of the plasma density [17,18]. However, this frequency downshift is through a mode conversion process which occurs even in a lossless plasma and is different from the process considered in the present work. In many practical situations, the created plasmas are collisional. The collisionality of the plasma changes the real part of the dispersion relation of the wave from $\omega=(\omega_{pe}^2+k^2c^2)^{1/2}$ to

$$\omega\approx(\omega_{pe}^2+k^2c^2-\nu^2)^{1/2}\ ,$$

where ν is the electron collision frequency. Moreover, if the wave is strong enough to cause ionization, the ionization loss of the wave also gives rise to an effective collision frequency modifying the dispersion relation of the wave. It explains qualitatively why a significant frequency downshift to the interacting wave can also result. However, the actual mechanism is much more mathematically involved, as will be shown later. In the present work, the role of electron collision frequency in causing frequency downshift is identified by a systematic study, including experimental demonstration, theoretical formulation, and computer simulation, of high-power EM pulse propagation in a self-generated plasma.

The experiment of pulse propagation is conducted in a vacuum chamber filled with dry air. The chamber is made of a 2-ft cube of Plexiglas. A microwave pulse is fed into the cube through an *s*-band microwave horn placed at one side of the chamber. A second *s*-band horn placed at the opposite side of the chamber is used to receive the transmitted pulse. The spectra of the incident pulse and the transmitted pulse are then compared. The microwave power is generated by a magnetron tube which is capable to producing 1 MW peak output power at a central frequency of 3.27 GHz. The tube is driven by a pulse-forming network (PFN) having a pulse width of 1 μs and a repetition rate of 40 Hz. The experimental setup is the same as that used in our previous work [15].

The electron–neutral-gas collision frequency ν is given by $C(p)\times10^9\sqrt{T_e}s^{-1}$, where T_e is the electron temperature measured in eV and $C(p)\sim6p$ is a function of the background pressure p measured in torr. The air pressure in the chamber is in the range 0.2 to 1 Torr and the electron temperature measured by a double probe using the time sampling method is in the range 1 to 2 eV for the microwave power employed. In order to avoid the undesired boundary effect, i.e., overionization to cause cutoff reflection of the incident pulse, the power of the incident pulse is limited to no more than 50% above the

breakdown threshold power level. Consequently, the ionization frequency of the background gas is of the same order of magnitude as the electron–neutral-gas collision frequency in the present experiment. Thus, the amount of frequency upshift and downshift will be of the same order of magnitude and the cause of frequency downshift can be examined conveniently.

Shown in Figs. 1(a)–1(d) is a sequence of photos which record the frequency spectra of incident and transmitted pulses in the same photo for four different incident power levels: $1.08P_c$, $1.14P_c$, $1.32P_c$, and $1.37P_c$, where P_c is the breakdown threshold power. The peaks of the spectra of the transmitted pulses in Figs. 1(a) and 1(b) are shown to be upshifted from the carrier frequency 3.27 GHz of the incident pulses. The upshifted quantities are 0.26 and 0.45 MHz, respectively. Moreover, the photo in Fig. 1(b) shows that the spectrum of the transmitted pulse starts to break up and a downshifted component emerges. Figures 1(c) and 1(d) show an even more pronounced effect. The spectra of the transmitted pulses have two clear peaks. One is upshifted and the other one downshifted from the single peak location of the incident pulse. The amount of frequency downshift is also comparable to that of upshifted frequency in both cases. In the following a theoretical model describing the experiment of pulse propagation in a self-generated plasma is developed. This model is used first to perform computer simulation of the experiment for validating the theoretical model and then to further carry out computer experiments for identifying the role of collisional loss in the fre-

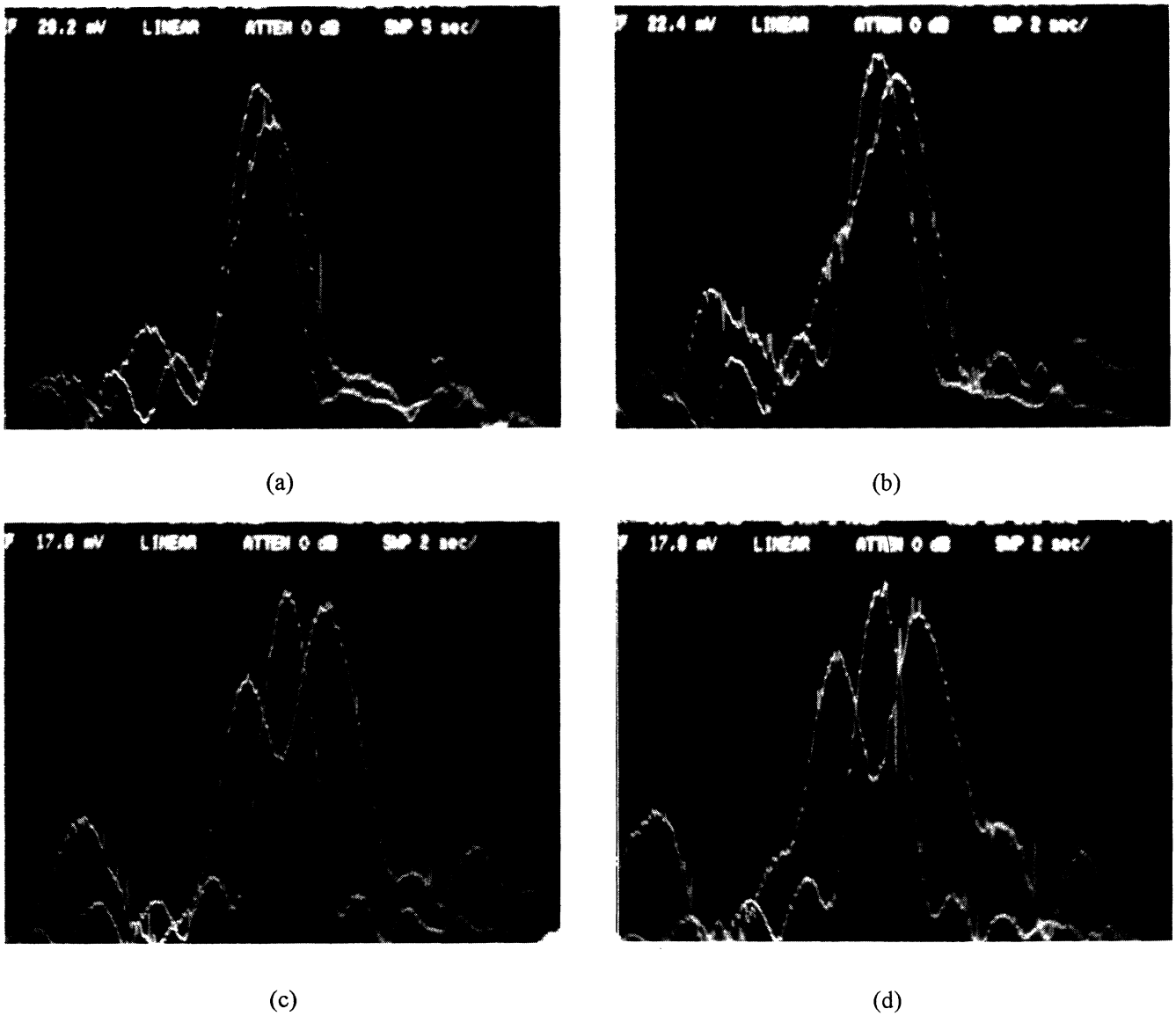

FIG. 1. Amplitude spectra of the incident and transmitted microwave pulses for four different powers: (a) $P=1.08P_c$, (b) $P=1.14P_c$, (c) $P=1.32P_c$, and (d) $P=1.37P_c$. The ranges of the vertical axes for the spectra of the incident pulses from (a) to (d) are 3.16, 3.16, 39.8, and 39.8 mV, respectively. On the other hand, the values 28.2, 22.4, 17.8, and 17.8 mV on top of the photos are the ranges of the vertical axes for the spectra of the transmitted microwave pulses. All the spectra are recorded with the same amount of attenuation.

quency downshift phenomenon.

The propagation of an EM pulse that is intense enough to cause the breakdown of the background gas is considered. The plasma along the trail of the pulse is generated by the pulse. The rate equation for electron density n_e generated by the pulse is given by

$$\frac{\partial}{\partial t}n_e=(\nu_i-\nu_a)n_e-\gamma n_e^2 , \tag{1}$$

where ν_i, ν_a, and γ are the ionization frequency, attachment frequency, and recombination coefficient, respectively.

The electron momentum equation including the momentum loss attributed to both elastic and inelastic collisions is

$$\frac{\partial}{\partial t}(n_e v_e)=-n_e eE/m_e-(\nu+\nu_a+\gamma n_e+\eta\nu_i)n_e v_e , \tag{2}$$

where $\eta=(\varepsilon_i/E_{\rm KE})^{1/2}$, the square root of the ratio of the ionization energy $\varepsilon_i\sim 12$ eV of the background gas to the electron average kinetic energy $E_{\rm KE}\sim(\varepsilon+0.03)$ eV, gives a measure of effective momentum loss in each ionization event; ε as defined later is the ratio of the field amplitude of the pulse to the breakdown threshold field of the background gas.

The governing wave equation derived from Maxwell's equations using (1) and (2) is

$$\left[\frac{\partial^2}{\partial t^2}-c^2\frac{\partial^2}{\partial z^2}+\omega_{pe}^2\right]E(z,t)=-\nu_1\omega_{pe}^2(m_e/e)v_e(z,t) , \tag{3}$$

where the relation $\mathbf{J}=-en_e\mathbf{v}_e$ has been used, ν is the electron–neutral-gas collision frequency,

$$\omega_{pe}=(4\pi n_e e^2/m_e)^{1/2} ,$$

and

$$\nu_1=\nu+\nu_a+\gamma n_e+\eta\nu_i .$$

Using the relation in (1), (2) is reduced to

$$\frac{\partial}{\partial t}v_e=-eE/m_e-\nu_2 v_e , \tag{4}$$

where $\nu_2=\nu+(\eta+1)\nu_i$.

Equations (1), (3), and (4) give a self-consistent description of pulse propagation in an ionizing background. They are coupled together through the ionization frequency ν_i which is modeled to be [19]

$$\nu_i=3.83\times 10^2\nu_a[\varepsilon^{3/2}+3.94\varepsilon^{1/2}]\exp[-7.546/\varepsilon] , \tag{5}$$

where $\varepsilon=|A/A_{\rm th}|$; A is the real wave field amplitude and defined through the expression of wave field $E(z,t)=A(z,t)e^{-i\phi(z,t)}+$c.c., with c.c. representing the complex conjugate; and the breakdown threshold field amplitude

$$A_{\rm th}\sim 18p(1+\omega^2/\nu^2)^{1/2}\ \text{V/cm}$$

for a continuous wave (cw) in which p is the background pressure measured in Torr and ω is the frequency of the wave. If the pulse is not too short, i.e., containing several oscillations, the variation of the amplitude function $A(z,t)$ in space and time is much slower than that of the phase function $\phi(z,t)$. It is also true to the counterparts of the corresponding velocity response, which is expressed accordingly as

$$\mathbf{V}_e=V(z,t)e^{-i\phi(z,t)}+\text{c.c.}$$

Hence, $|\partial\ln A/\partial t|$ and $|\partial\ln V/\partial t|\ll|\partial\phi/\partial t|$, and $|\partial\ln A/\partial z|$ and $|\partial\ln V/\partial z|\ll|\partial\phi/\partial z|$. These inequalities can be employed to simplify the analysis. In addition, the forward-scattering approximation leading to the definition of local frequency $\omega=\partial\phi/\partial t$ and local wave number $k=-\partial\phi/\partial z$ will also be used to simplify further the analysis. This approximation is justified because only the portion of the pulse propagating in the forward direction is of interest.

Using these approximations and the approximate result

$$V(z,t)\sim -ieA(z,t)/m(\omega+i\nu)$$

derived from (4), (3) is reduced to

$$\frac{\partial(\omega A^2)}{\partial t}+\frac{\partial(kc^2A^2)}{\partial z}=-\omega_{pe}^2\nu_1\omega A^2/(\omega^2+\nu_2^2) \tag{6}$$

and

$$\omega^2-k^2c^2=\omega_{pe}^2[1-\nu_1\nu_2/(\omega^2+\nu_2^2)] . \tag{7}$$

Equation (6) is the continuity equation for the energy density of the pulse, while (7) is the local dispersion relation. ω and k are related by

$$\frac{\partial\omega}{\partial z}+\frac{\partial k}{\partial t}=0 . \tag{8}$$

It should be noted that (7) has the conventional meaning as the real part of the dispersion relation only if n, ω, and k are constant parameters. In the present case, n, ω, and k are all space-time dependent functions. Hence, the spectrum and the damping rate of the pulse have to be determined by the set of equations (1), (5), and (6)–(8). In other words, (7) alone cannot provide adequate information on the space-time evolution of the spectrum of the pulse.

Taking the partial time derivative of (7) and using the relation (8) to simplify the result yields

$$\frac{\partial\omega^2}{\partial t}+v_g\frac{\partial\omega^2}{\partial z}=\{[1-\nu_1\nu_2/(\omega^2+\nu_2^2)]/[1-\omega_{pe}^2\nu_1\nu_2/(\omega^2+\nu_2^2)^2]\}\frac{\partial}{\partial t}\omega_{pe}^2 , \tag{9}$$

where $v_g = \partial\omega/\partial k$ is the group velocity of the pulse.

Equations (1), (6), and (9) together with (5) form a complete set of modal equations describing the amplitude and phase variation of a one-dimensional pulse propagating in a self-generated plasma. The ionization frequency ν_i provides the coupling between Eqs. (1) and (6).

A numerical program using the LSODE package [20] is developed for solving the set of modal equations. The numerical analysis is first performed to simulate the experiment. The value $\nu_a = 1.2\times10^4$ sec^{-1} determined experimentally, and the dependence of $\nu = 4\times10^9$ sec$^{-1}\sqrt{T_e}$, where $T_e = (\varepsilon + 0.03)$ eV, are used in the numerical simulations. The ν value suggests that the background pressure is around 0.7 Torr. The frequency spectra of the transmitted pulses corresponding to the incident pulses of $1.08P_c$, $1.14P_c$, $1.32P_c$, and $1.37P_c$ are evaluated. In numerical simulations, the following initial and boundary conditions are employed:

$$n(z,t=0) = n_0 ,$$

$$A(z=0,t) = A_0 \exp\{-0.5[(t-t_0)/t_0]^{10}\} \times \exp[0.15\sin(t/t_0 + 0.35)] ,$$

and

$$\omega(z=0,t) = \omega_0 = \omega(z,t=0) ,$$

where $n_0 = 10^6$ cm^{-3} is the background electron density maintained by the repetitive microwave pulse, $t_0 = 0.5$ μs, and $\omega_0/2\pi = 3.27$ GHz. The results are shown in Figs. 2(a)–2(d) for comparison with the corresponding experimental results shown in Figs. 1(a)–1(d).

Figures 2(a) and 2(b) also show that the transmitted pulses are frequency upshifted. The amounts of frequency upshifts are 0.23 and 0.47 MHz, which are in good agreement with the experimental results of 0.26 and 0.45 MHz. The spectral breaking phenomenon shown in Figs. 1(c) and 1(d) also appears in the results of numerical simulation as shown in Figs. 2(c) and 2(d). This consistency further validates the model.

We now perform a computer experiment to verify the cause by collision to frequency downshift. This is done by multiplying a variable parameter ξ to the electron–neutral-gas collision frequency ν in Eqs. (1), (6), and (9) and varying ξ from 0.5 to 2. In general, ν_i and ν_a are proportional to ν; however, their relationships are removed artificially in the computer experiment. In other words, only the electron–neutral-gas collision frequency ν is varied artificially for a fixed background condition. In doing so, the role of ν in the frequency downshift result may be identified unambiguously.

Presented in Fig. 3(a) are the dependencies of the amounts of frequency downshift $-\Delta f_d$ on ξ for five

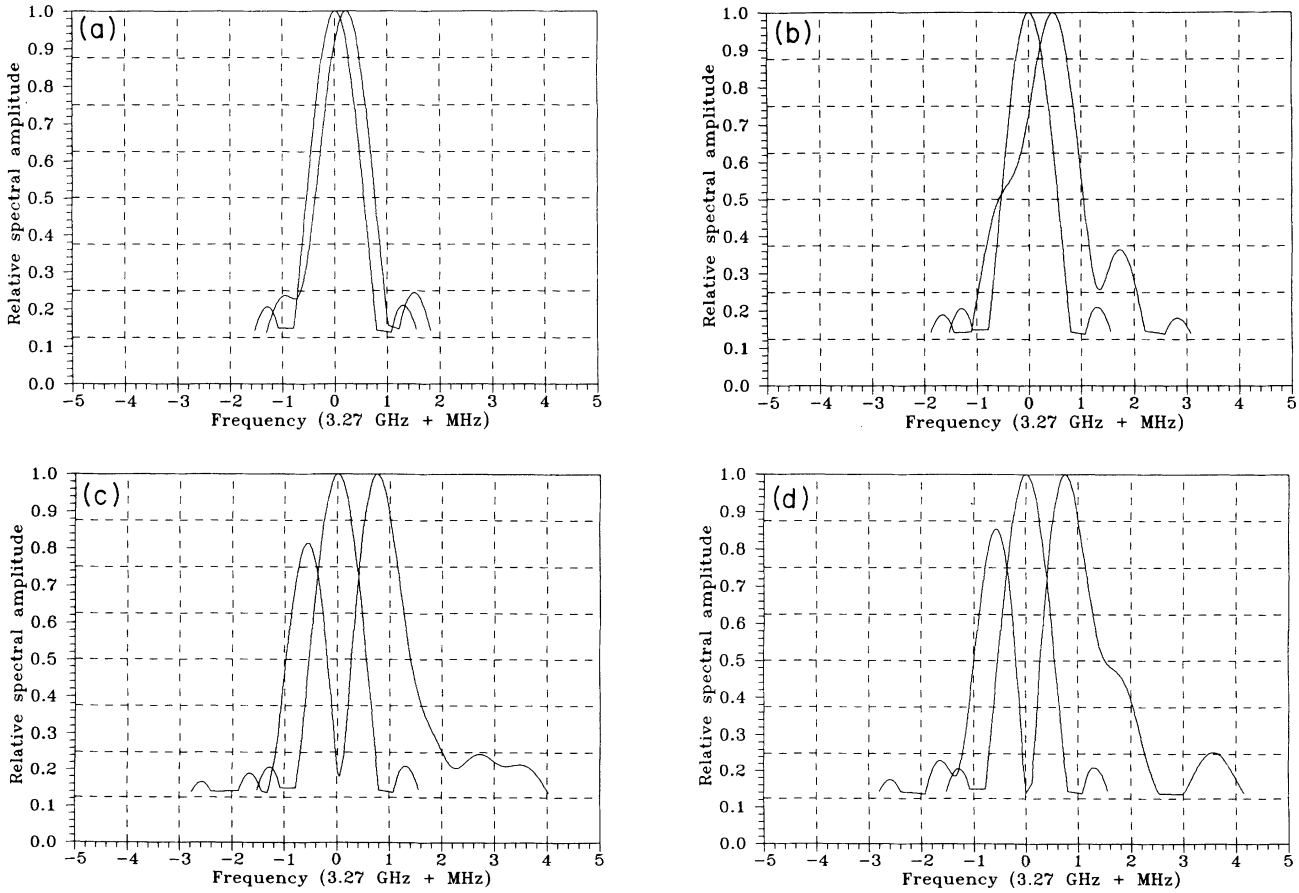

FIG. 2. Amplitude spectra of the incident and transmitted microwave pulses calculated from the numerical simulations of the experiments conducted for Fig. 1: (a) $P = 1.08P_c$, (b) $P = 1.14P_c$, (c) $P = 1.35P_c$, and (d) $P = 1.37P_c$.

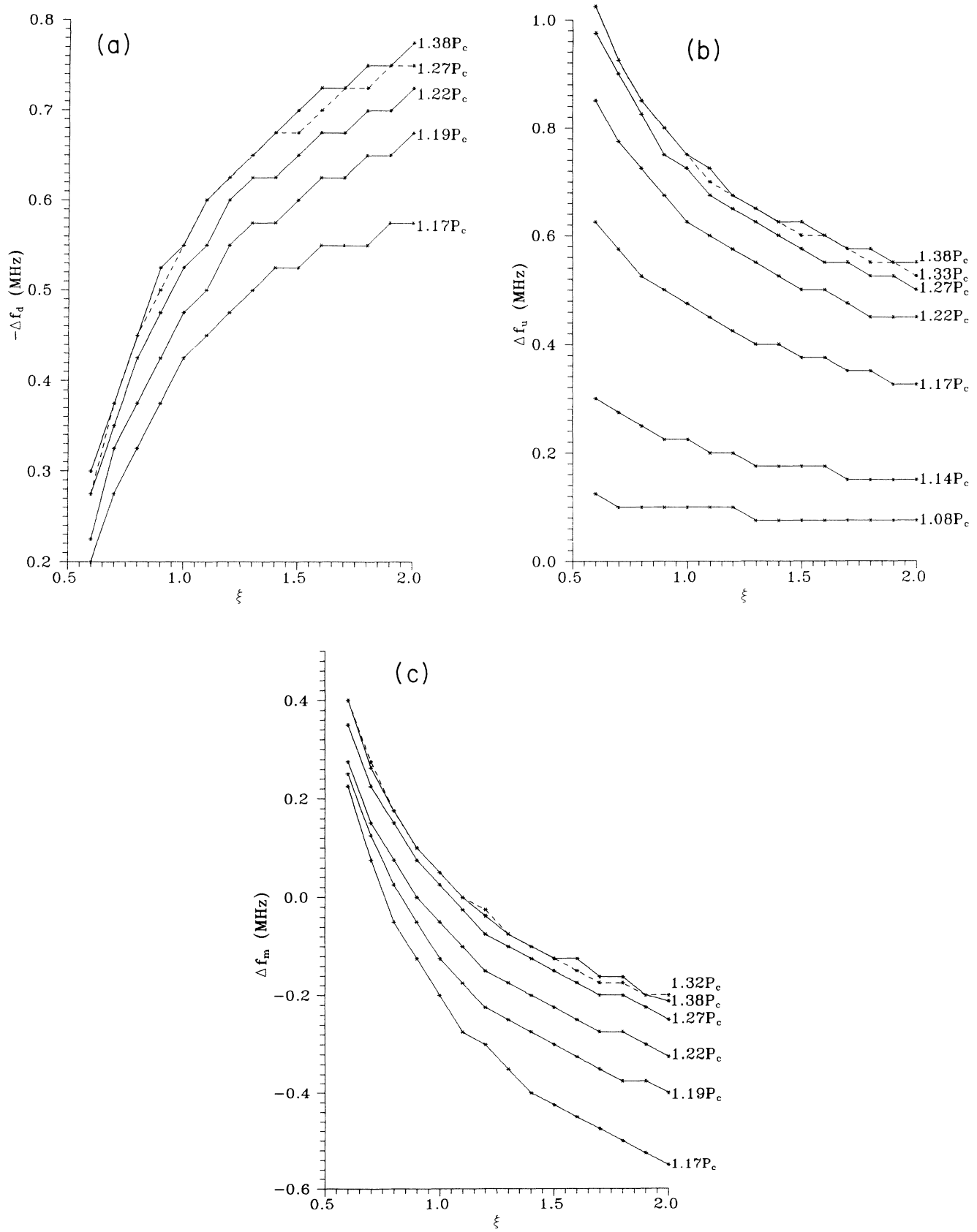

FIG. 3. The results of the computer experiments: (a) The amount of frequency downshift $-\Delta f_d$ vs the parameters ξ and P, (b) the amount of frequency upshift Δf_u vs the parameters ξ and P, and (c) the shift Δf_m of the frequency f_m of the spectral minimum between the two spectral peaks vs the parameters ξ and P.

different incident power levels. A monotonic increase of $-\Delta f_d$ with ξ is observed for all cases. $-\Delta f_d$ also varies with the power of the incident pulse, P. It increases with P and then reaches a saturation level, as manifested by the overlap of the two curves corresponding to $P=1.27P_c$ and $1.38P_c$. On the other hand, the dependencies of the amounts of frequency upshift Δf_u on ξ and P presented in Fig. 3(b) show that Δf_u decreases monotonically with ξ, but increases monotonically with P to a saturation level. The frequency f_m of the minimum between the two peaks of the spectrum of the transmitted pulse also varies with ξ and P. The dependencies of $\Delta f_m (=f_m - f_0)$ on ξ and P are presented in Fig. 3(c). Similar to Δf_u, Δf_m decreases with ξ and increases with P to a saturation level. These results clearly demonstrate that ξ plays an important role in determining the frequency shift—in particular, in introducing the downshifted frequency components in the spectrum of the transmitted pulse.

In summary, we have demonstrated experimentally and in computer simulation that the interaction between an EM wave and a fast growing plasma can also generate frequency downshifted spectral components if the plasma is collisional. Physically, this is realized by the fact that electron collisions reduce the phase velocity of the wave in the plasma as indicated by the dispersion relation. The increasing dependence of frequency downshift on the electron–neutral-gas collision frequency observed in the computer experiments suggests that the frequency downshift phenomenon observed in the laboratory experiments is indeed caused by the collisionality of the plasma.

The spectral breaking phenomenon shown in Figs. 1(c) and 1(d) suggests a potential application for devising a plasma optical switch. By using a receiver with a narrow band detector centered at the carrier frequency of the incident pulse, the received power can be reduced suddenly by increasing the incident power to exceed a critical level. Thus, an on-off switch can be made by changing the power of the incident pulse. The plasma may also be generated by external means, so that a low power pulse can serve for this application.

One of the authors (S.P.K.) would like to acknowledge a useful conversation with Dr. Paul Bolton of the Lawrence Livermore National Laboratory. This work was supported by the U.S. Air Force System Command, the Air Force Office of Scientific Research, Grant No. F49620-94-1-0076. The work of G.S. was supported by the U.S. Department of Energy, Office of Basic Energy Sciences.

[1] S. C. Wilks, J. M. Dawson, and W. B. Mori, Phys. Rev. Lett. **61**, 337 (1988).
[2] S. C. Wilks, J. M. Dawson, W. B. Mori, T. C. Katsouleas, and M. E. Jones, Phys. Rev. Lett. **62**, 2600 (1989).
[3] A. V. Kim, S. F. Lirin, A. M. Sergeev, E. V. Vanin, and L. Stenflo, Phys. Rev. A **42**, 2493 (1990).
[4] W. B. Mori, Phys. Rev. A **44**, 5118 (1991).
[5] E. Esarey, G. Joyce, and P. Sprangle, Phys. Rev. A **44**, 3908 (1991).
[6] S. C. Rae and K. Burnett, Phys. Rev. A **46**, 1084 (1992).
[7] E. Yablonovitch, Phys. Rev. Lett. **31**, 877 (1973); **32**, 1101 (1974).
[8] S. P. Kuo, Phys. Rev. Lett. **65**, 1000 (1990).
[9] C. Joshi, C. E. Clayton, K. March, D. B. Hopkins, A. Sessler, and D. Whittum, IEEE Trans. Plasma Sci. **18**, 814 (1990).
[10] R. L. Savage, Jr., C. Joshi, and W. B. Mori, Phys. Rev. Lett. **68**, 946 (1992).
[11] R. Sauerbrey, F. P. Schafer, U. Teubner, J. Bergmann, S. Szatmari, and S. P. L'Blanc, *X-ray Laser,* edited by E. E. Fill, IOP Conf. Proc. No. 125 (AIP, New York, 1992), p. 205.
[12] S. P. Kuo and A. Ren, IEEE Trans. Plamsa Sci. **21**, 53 (1993).
[13] W. M. Wood, C. W. Siders, and M. C. Downer, IEEE Trans. Plasma Sci. **21**, 20 (1993).
[14] S. P. LeBlanc, R. Sauerbrey, S. C. Rae, and K. Burnett, J. Opt. Soc. Am. B **10**, 1801 (1993).
[15] S. P. Kuo and A. Ren, J. Appl. Phys. **71**, 5376 (1992).
[16] V. B. Gildenburg, V. A. Krupnov, and V. E. Semenov, Pis'ma Zh. Tekh. Fiz. **14**, 1695 (1988) [Sov. Tech. Phys. Lett. **14**, 738 (1988)].
[17] D. K. Kalluri and V. R. Goteti, IEEE Trans. Plasma Sci. **18**, 797 (1990).
[18] D. K. Kalluri, IEEE Trans. Plasma Sci. **21**, 77 (1993).
[19] Yu. A. Lupan, Zh. Tekh. Fiz. **46**, 2321 (1976) [Sov. Phys. Tech. Phys. **21**, 1376 (1976)].
[20] R. F. Sincovec and N. K. Madsen, ACM Trans. Math. Software E **1**, 232 (1975).

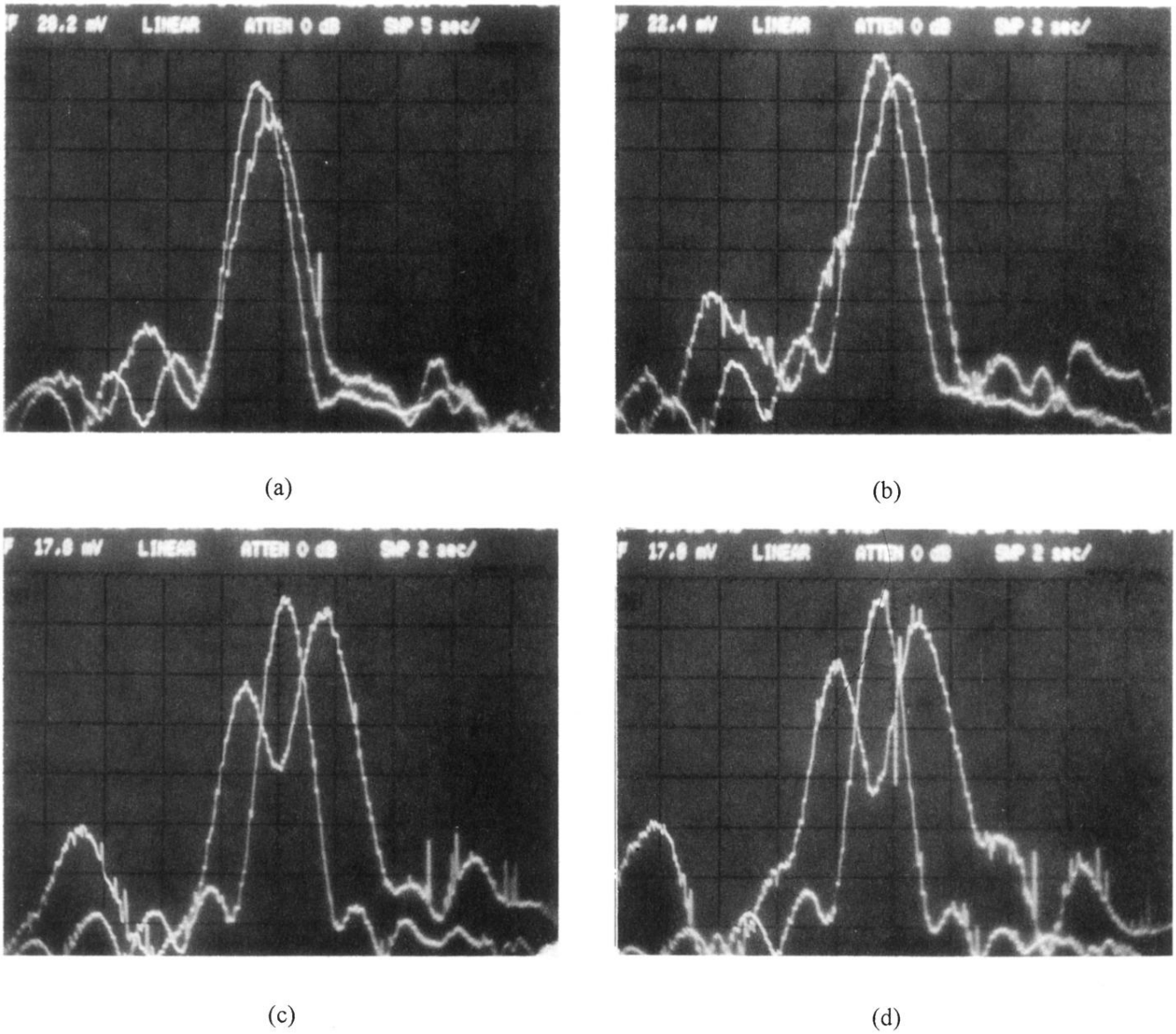

(a) (b)

(c) (d)

FIG. 1. Amplitude spectra of the incident and transmitted microwave pulses for four different powers: (a) $P=1.08P_c$, (b) $P=1.14P_c$, (c) $P=1.32P_c$, and (d) $P=1.37P_c$. The ranges of the vertical axes for the spectra of the incident pulses from (a) to (d) are 3.16, 3.16, 39.8, and 39.8 mV, respectively. On the other hand, the values 28.2, 22.4, 17.8, and 17.8 mV on top of the photos are the ranges of the vertical axes for the spectra of the transmitted microwave pulses. All the spectra are recorded with the same amount of attenuation.